Sports Engineering
https://doi.org/10.1007/s12283-019-0309-2

ORIGINAL ARTICLE

Image-based center of mass estimation of the human body via 3D shape and kinematic structure

Tomoya Kaichi[1] · Shohei Mori[1,2] · Hideo Saito[1] · Kosuke Takahashi[3] · Dan Mikami[1,3] · Mariko Isogawa[3] · Yoshinori Kusachi[3]

Abstract
This paper presents a method to estimate a time-sequential trajectory of the center of mass (CoM) of an athlete from a multi-view set of cameras. Collecting the CoM typically requires large-scale measuring systems or attaching sensors to the athletes. To mitigate such hardware limitations, the present study takes a multi-view video-based approach. The proposed method reconstructs subjects' voxels from a set of multi-view frames and weights each voxel with body part-dependent weights to calculate a CoM. Our results, using real data measured in a studio, showed that the proposed method can estimate CoM within 20 mm concerning center of pressure measures.

Keywords Center of mass · Multi-view videos · Visual hull · Multi-view human pose estimation

1 Introduction

Measuring athletes' dynamic center of mass (CoM) plays an important role in many sports applications. The ability to balance (i.e., *the ability to perform a task while maintaining or regaining a stable position* [34]) affects the performance of athletes and the risk for sport-related injuries [16, 17]. The movements for the control of balance have been described in a single-dimensional space related to the horizontal position of the body's CoM [26]. Indeed, the 3D CoM affects the performance of the athletes in some sports [15, 18, 32]. Analysis of the CoM is also used to develop sports devices, such as snowboards and poles of pole vaulting [2, 12].

Many researchers, therefore, have attempted to develop methods to estimate 3D CoM, but most of them have relied on the performance of hardware. For example, classical methods have used motion capture systems (MoCap) and force plates to measure the human body's CoM [6, 21]. However, these systems are designed only for special environments, such as research labs and studios, and markers are attached to athletes. While such systems are reliable and accurate, casual CoM measuring has great potential. For example, such systems could be used to collect CoM data during competitive team games. Thus, measuring CoM under limited hardware resources has been of great interest in this area [14, 25]. However, prior measurement for personalizing the weight of the body segments is required for such systems to achieve the same accuracy as that of [6, 21].

From this background, we propose a 3D CoM estimation method for athletes that only relies on a set of multi-view cameras. The multi-camera setting is motivated by many existing image-based approaches which analyze sports motion in real game [28] and in the situations where it is difficult to wear devices on players' body [4, 36].

Considering our targets are sports players, our method must meet the following conditions:

1. the proposed method works in outside games,
2. with no wearable devices attached, and
3. with no prior personalization.

To satisfy these conditions, we propose estimating the CoM using multi-view RGB images only. First, we reconstruct a 3D model of the subject's body using multi-view RGB images. The 3D model is divided into nine body parts, and

✉ Tomoya Kaichi
kaichi@hvrl.ics.keio.ac.jp

[1] Keio University, 3-14-1, Hiyoshi, Kohoku-ku, Yokohama, Kanagawa 223-8522, Japan

[2] Graz University of Technology, Graz, Austria

[3] NTT Media Intelligence Laboratories, Yokosuka, Japan

Published online: 01 August 2019

weights, depending on the body parts, are assigned to each part. Then the weighted average of the parts are used to calculate the whole body's CoM. Since the proposed method uses only RGB images, outdoor CoM estimation is achieved (condition 1) and wearable devices are not necessary (condition 2). Moreover, 3D shape reconstruction of the subject's body handles the differences in individuals' figures when calculating the CoM (condition 3). The proposed approach is the first attempt toward an end-to-end automated process for 3D CoM estimation using image inputs only, taking the volumetric properties of the measured athlete into account.

In this paper, we conducted two experiments. We evaluated the accuracy of the CoM estimation in static posture, and discuss the effects of the number of cameras on the CoM estimation. For the second, we demonstrated the applicability of the proposed method utilizing the cooperation of professional and amateur baseball batters assuming a setup of an actual game.

2 Related work

In this section, we review previous works on CoM estimation as well as prior researches of vision-based sports motion analysis. Table 1 summarizes the possible situations for using the proposed methods in actual games and the applicability of the conventional and the proposed methods.

The force plate approaches measure ground reaction forces to calculate CoM motion based upon Newton's second law, which states that the net external force acting upon a body is equal to its mass multiplied by its acceleration. The motion capture approaches use kinematic data acquired from markers that are placed on the body, incorporating an anthropometric model to calculate the segmental CoM positions. Saini et al. compared the accuracy of these two simple methods and confirmed that they could estimate CoM when the subjects moved slowly [27]. Carpentier et al. proposed a method to estimate the CoM by combining the data from force plates and motion capture systems [6]. They reduced sensor noise using data fusion based on complementary filtering. However, force plates can only be used when the body is touching the ground. In addition, it is difficult to move force plates and motion capture systems, and these devices limit the range of movement of the subject.

To relax the restrictions on the measuring environments, González et al. proposed the use of Kinect and Wii balance board together [13, 14]. They reported that the method could estimate CoM with accuracy close to that of a Vicon motion capture system by personalizing each part of the human body beforehand [14]. In contrast to acquiring the skeleton of the body from Kinect, some works recover the body shape with depth sensors [3, 8]. However, the measurement accuracy of the Kinect decreases outdoors.

Wearable motion capture systems have been used for motion analysis for approximately a decade. They obtain body segments with fewer restrictions concerning the environment [7, 30]. Najafi et al. estimated the trajectory of CoM during a golf club swing using wearable sensors; they showed that wearable technologies, based on inertial sensors, are a viable option for assessing dynamic postural control in complex tasks [25]. Wearable sensors can be used in both indoor and outdoor situations. However, as most sports forbid the wearing of what may harm players during games, wearable sensors cannot be used to estimate players' CoM during actual activities.

To the best of our knowledge, only the work by Dawes et al. [11] estimates the CoM from images. They have taken a skeleton-based approach using manually selected joint locations in images. On the other hand, full body motion analysis from images are developed for various sports scenes [4, 19, 36]. Zecha et al. estimated the motion of a swimmer under water [36]. Sheets et al. reconstructed a player's body during a tennis serve using multiple cameras [28]. Some works recover the 3D shape of human in motion with visual hull and explored the optimal camera configuration [9, 24]. Motivated by their volumetric and kinematic analyses, the proposed framework estimates the CoM combining reconstructed model of a player with kinematic information obtained from images.

Table 1 The applicability of the conventional and the proposed methods

Condition (Sec. 1)	MoCap	Depth sensors	Wearable MoCap	Ours
1. Outdoor	No	No	Yes	Yes
2. Wearing devices	Yes	No	Yes	No
3. Personalization	No	No	Required	No

3 Methods

3.1 Overview

The proposed method estimates the CoM of a person in a process using N calibrated cameras ($N \geq 2$). A global summary of the proposed process is shown in Fig. 1. The input consists of only RGB images taken from multiple viewpoints. Those images are used for 3D reconstruction of the body shape and a 3D kinematic structure estimation of the human body. Based on the joint positions obtained via the estimation of the body structure, the human body model is segmented into nine parts. Then the CoM is obtained by

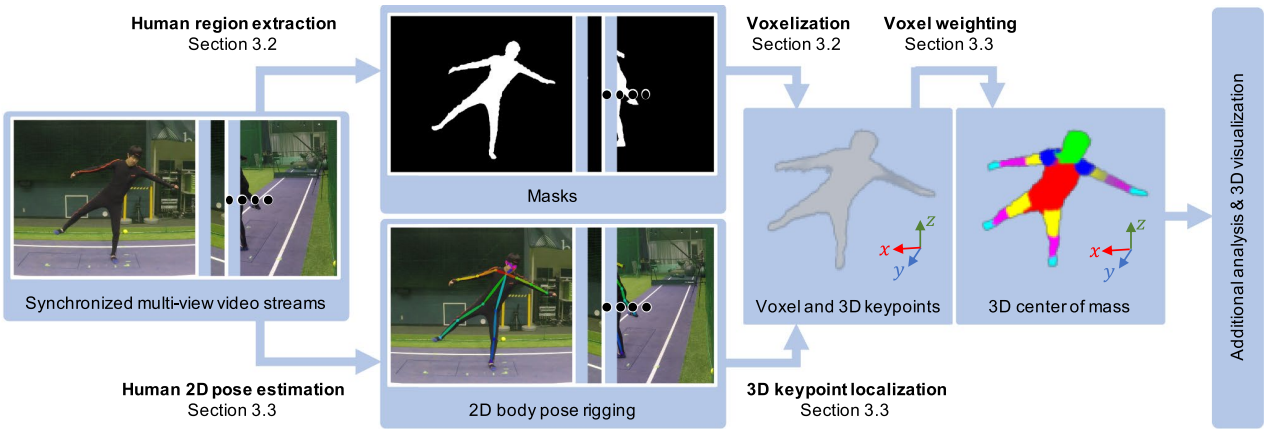

Fig. 1 An overview of the proposed CoM estimation using visual hull and body-part-dependent voxel-wise weighting

assigning a weight to each part of the human body, reported by [20].

3.2 3D reconstruction of the human body

The 3D human body is reconstructed using Martin's method [22]. We extract the subject's 2D silhouette from the input images (e.g., using [31]) and reproject the silhouettes into a 3D world. The common parts of the reprojected silhouette are the 3D shape of the body $\mathbf{V}$. $\mathbf{V}(\ni \mathbf{v}_j)$ denotes a set of voxels, where each voxel element $\mathbf{v}_j$ contains 3D positional information. In the case that the subject holds tools, we have a choice of whether to include or exclude the tools from the following CoM calculation. To retrieve a precise 3D model, cameras need to be arranged to observe the voxel space from various angles [23]. By reconstructing the 3D shape of the subject's body, it is possible to reflect any individual's unique figure.

3.3 Human kinematic structure estimation

If the frame of reference is at the center of mass, CoM is the unique position at which the weighted position vectors of all the parts of a system add up to zero. Because each body part has a different density [1], assigning the appropriate weight to each part will lead to a more accurate CoM estimation. As shown in Fig. 2, the 3D model reconstructed in Sect. 3.2 is divided into nine parts: head, body, shoulder, back arm, forearm, hand, thigh, calf, and foot.

We obtain 2D key points, which represent the joints and the face of an individual, from the input images by applying the method of Cao et al. [5]. By applying the direct linear transform to each 2D key point $\mathbf{q}$ to triangulate them, we obtain the 3D position $\mathbf{p}$ of each $\mathbf{q}$.

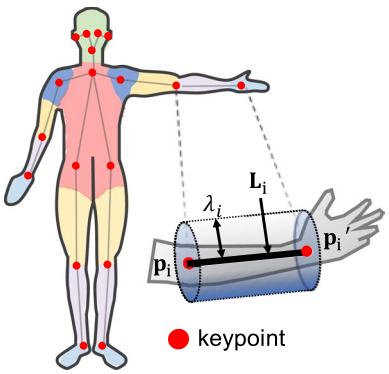

Fig. 2 Variables in a segmented part

Algorithm 1: Proposed segmentation procedures

$\mathbf{V}_i$: A part of 3D human body model $\mathbf{V}$
$\mathbf{v}_j$: A voxel costituting the 3D model $\mathbf{V}$
$\mathbf{p}_i$, $\mathbf{p}'_i$: Keypoints that divide $\mathbf{V}$ into $\mathbf{V}_i$
$\mathbf{L}_i(\mathbf{p}_i, \mathbf{p'}_i)$: Line segment between $\mathbf{p}_i$ and $\mathbf{p}'_i$

```
foreach v_j do
    foreach L_i(p_i, p'_i) do
        D_i ← CalcDistance(v_j, L_i)
    end
    if Min(D_i) < λ_i then
        stock v_j to V_i
    else
        remove v_j
    end
end
```

As shown in Fig. 2, the 3D model $\mathbf{V}$ is segmented into $\mathbf{V}_i$ $(0 \leq i < 9)$ based on the distance between the line segments $\mathbf{L}_i$ connecting the adjacent key points $\mathbf{p}$ and each voxel $\mathbf{v}_j$. Algorithm 1 shows the segmentation procedure. A voxel $\mathbf{v}_j$

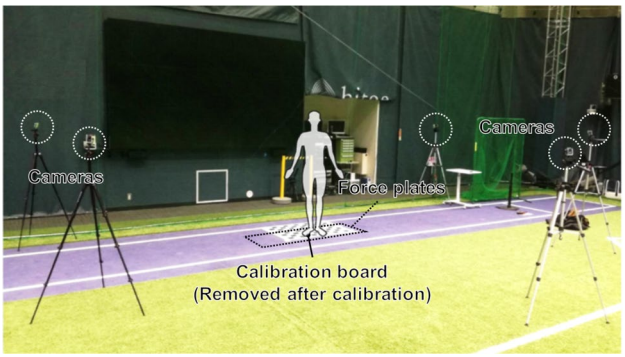

Fig. 3 Experimental setup of a static scene

which exists within a distance λ_i from $\mathbf{L}_i$ is classified as $\mathbf{V}_i$. A voxel $\mathbf{v}_j$ located in the common area of two or more body parts is classified as the part with the smaller distance. All voxels $\mathbf{v}_j$ that are not classified as any body part are removed. The threshold λ_i is manually set to be large to not remove the body parts. The segmented model is weighted based on the weight of each part of the human body, as reported by de Leva [20]. The overall CoM of the human body $\mathbf{C}$ is computed via

$$\mathbf{C} = \frac{1}{M}\sum_{i=1}^{M} w_i \mathbf{v}_i, \tag{1}$$

where M denotes the total number of voxels and w_i represents the weight assigned to $\mathbf{V}_i$.

4 Experiments

This section provides two performance evaluations of the proposed method using real data. First, we compare three methods to show that the proposed method outperforms the others concerning accuracy in terms of the center of pressure (CoP) error metric [35]. Second, we present a 3D visualization of different performances and a comparison with the wearable sensor to demonstrate that the proposed method has the ability to provide meaningful 3D data for sports performance analysis.

4.1 Evaluating the CoM accuracy

4.1.1 Setups

As shown in Fig. 3, a force plate (TF-6090) and five cameras (GoPro, 30 fps, 1920 × 1080 resolution) were utilized in this evaluation. Internal and external camera parameters were obtained through off-line calibration with [37]. These cameras were set so as to surround the force plate at 0°, 45°, 100°, 260°, and 300° respectively, where 0° represented a face-on view of the subject, capturing the subject standing on the force plate. Three subjects (two male and one female) each stood on the force plate in four static postures: upright standing, single-leg standing, squatting, and bending forward. We extracted the human regions using a semi-automated manner implemented using GIMP2[1] in this experiment, to confirm the pixel mask.

To demonstrate the performance of the proposed method, we compared it with the following two methods:

Uniform: voxels with a uniform weight This method estimates the CoM as the center of a reconstructed 3D model, in which all parts are assigned a uniform weight. The CoM is computed by Eq. (1) with all $w_i = 1$.

Articulated: articulated joint model This method estimates the CoM as the center of the weighted articulated joint model. The CoM is computed by

$$C = \frac{1}{M'}\sum_{i=1}^{M'} w_i \boldsymbol{j}_i, \tag{2}$$

where $\boldsymbol{j}_i$ represents the 3D positions of the mid-points between two connected joints (e.g., we define the CoM of a left lower arm as a mid-point between a hand joint and an elbow joint), and M' denotes the number of the mid-points. The 3D joint positions are computed by triangulation with the 2D joints detected by [5].

The comparison with the uniform method clarifies the effectiveness of the proposed method for considering the weight of each part. A comparison with the articulated method reveals the influence of the volume of the human body on the CoM estimation accuracy.

[1] https://www.gimp.org/.

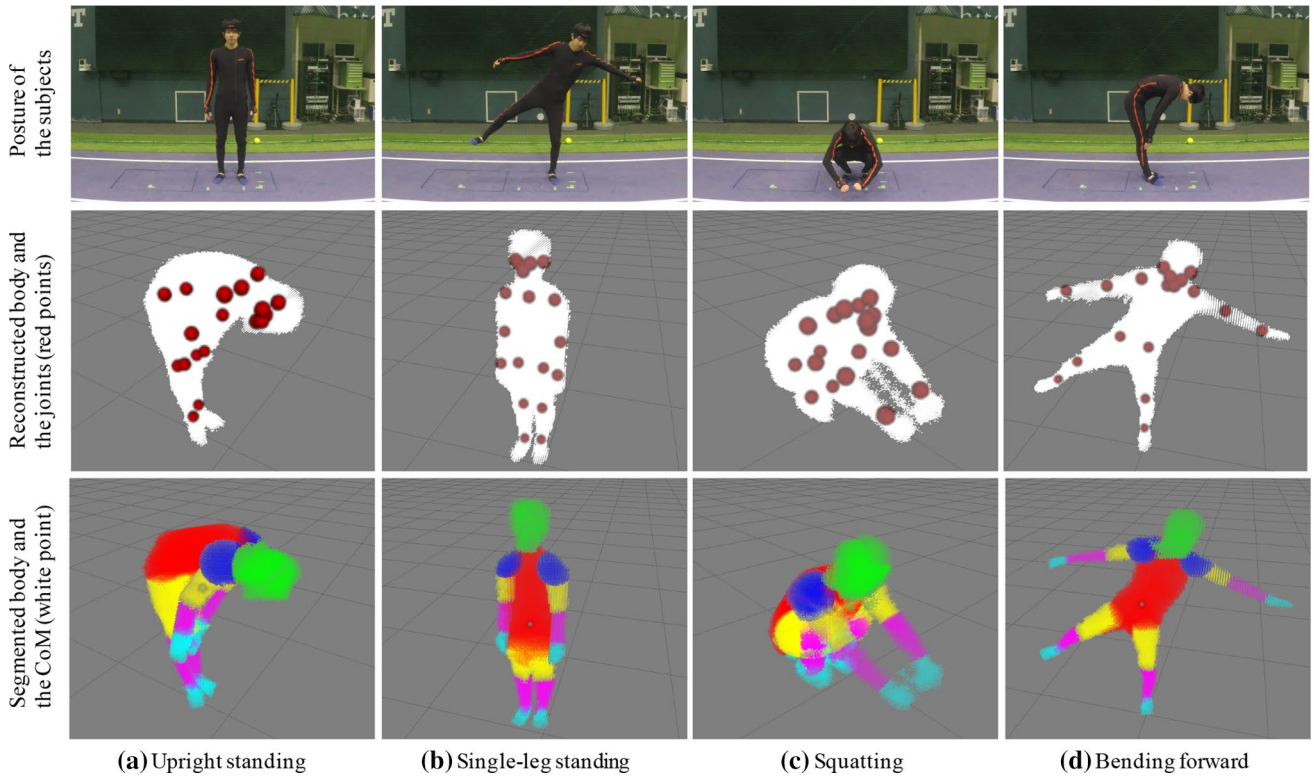

Fig. 4 The experimental results regarding static posture

In these evaluations, the CoM estimation error of each method was evaluated as the Euclidean distance of the 2D coordinates of the center of pressure $\boldsymbol{g}$, which represented the vertical projection of the estimated CoM as

$$E_{\mathrm{COP}} = |\boldsymbol{g} - \boldsymbol{g}_{\mathrm{f}}|, \tag{3}$$

where $\boldsymbol{g}_{\mathrm{f}}$ denotes the CoP estimated from a force plate. Note that the CoP estimated from a force plate is not always accurate, but we consider a force plate as providing a reference measurement for comparison with the proposed approach concerning static postures since a force plate is commonly used for measuring the CoP in the practical use of human motion measurement [29].

4.1.2 Results

Figure 4 shows the input images from one view (first row); the reconstructed 3D model, showing the joint positions (second row); the labeled 3D model, based on the joint positions and estimated CoM (third row). The results in the second and third row show that the estimated 3D joint positions were sufficient to assign each voxel to the appropriate body parts. The average estimation errors of each method are shown in Fig. 5. From these results, we observed that the proposed method outperformed the other methods and robustly estimated the CoM with errors of approximately 10 mm for the CoP in all postures.

In the case of standing upright, the precision of all methods was similar due to the symmetry of the posture. The precision of all methods was greater in the case of single-leg standing than in squatting and bending forward. This was caused by self-occlusions affecting the precision of both the reconstructed 3D model and the estimation of the joint positions. For example, the chest portion of the bending forward 3D model appeared to be thicker than the subject's chest. This was because the five cameras were placed at the

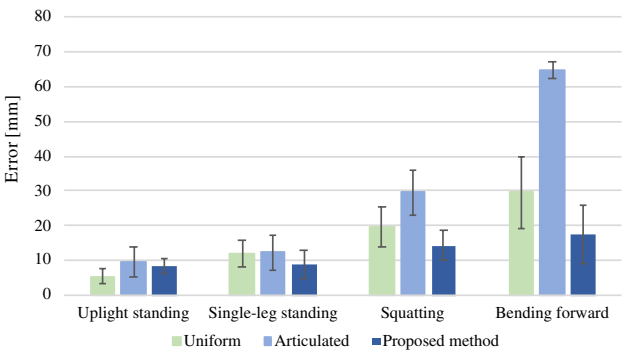

Fig. 5 The error between the reference value and the vertically projected CoM estimated by each method

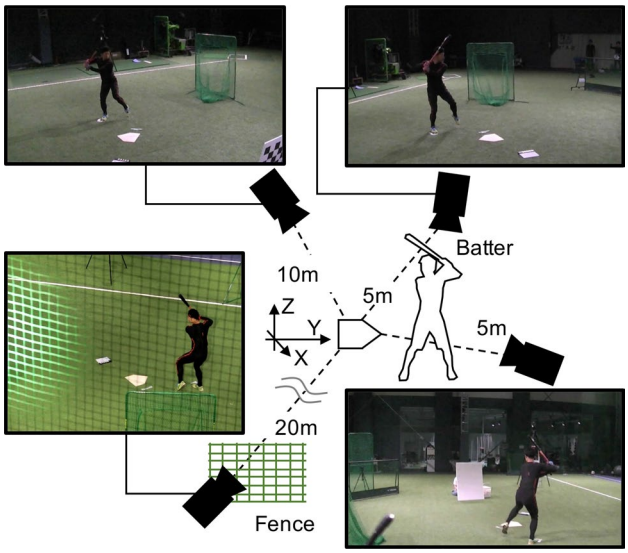

Fig. 6 The experimental setup for the CoM estimation of a baseball batter. All cameras were placed outside of the baseball field

same height (Fig. 3), and no cameras were able to observe under the chest. Actually, Mundermann et al. [23] found that cameras positioned in a geodesic dome configuration produce the best results to build visual hull model of human body. The reason for larger errors in the articulated method in squatting and bending forward posture, compared to the other methods, was self-occlusion as the authors reported. When there were only two or three cameras that could observe a joint, the error when projecting the joint in three dimensions tended to be large. While the articulated method used only joint positions that were ambiguous in an image, the proposed method maintained high accuracy even in self-occluded scenes using silhouettes.

4.2 CoM estimation for dynamic motion

4.2.1 Setups

Compared to the 2D CoP estimation approaches, utilizing a force plate, the vision-based approach including the proposed method could estimate 3D positions of the CoM, which is a significant advantage for analyzing a player's performance in a sports scene. In particular, it is known that CoP estimated with a force plate does not match the CoM projections when the subject is in motion [33]. Here, we demonstrated that the proposed method could estimate the 3D positions of CoM in such a challenging situation.

We placed the four cameras (three 640×360-resolution cameras and one 640×480-resolution camera) outside the baseball field, assuming that the proposed method would be used to observe a baseball batter. The camera position and example images taken with each camera are shown in Fig. 6. All cameras were fixed and pre-calibrated with [37]. We took 48 frames with 30 fps for each swing. The two subjects, an expert baseball batter and an amateur batter, swung a bat twice without batting a ball, assuming (a) an inside pitch and (b) an outside pitch. We extracted the subjects' regions in the same manner as in Sect. 4.1.1 (i.e., the bat held by the subject was excluded by masking it out).

The estimated time-sequential trajectory of the CoM was compared with the CoM trajectory calculated by a wearable sensor. The subjects wore Xsens MVN,[2] an inertial motion capture system generally used for human measurement on the field. We calibrated the MVN before swinging because inertial sensors require calibration on a regular basis to eliminate cumulative error. Note that the CoM from the wearable motion capture system was not a ground truth but a comparison to observe the validity of the CoM estimated by the proposed method.

4.2.2 Results

Figure 7 illustrates the 3D trajectories of the estimated CoM. The expert (the left graph of Fig. 7) and the amateur (the right graph) swung a bat twice. The red and blue trajectories correspond to the cases of (a) inside and (b) outside pitches, respectively. Since it was difficult to calibrate the coordinates of the proposed method's CoM and the coordinates of the MVN's CoM, the CoM sequence is plotted on a graph so that the sum of the distance of each CoM is minimized. The subjects were right-handed batters and assumed that a ball was coming from a negative to a positive direction along the x-axis.

In both the expert and the amateur swings, the CoM transitions of the proposed method drew almost the same trajectories as the CoM of the wearable sensor in the pulling arm phase and the swing phase. The mean absolute distance between the two CoM sequences was 25.2 mm. The trajectories against the inside and outside balls were almost the same when the arms were pulled back and gradually split in the swing phase. In the swing phase, it could be seen that the CoM for the outside pitch went through the outside compared to the CoM for the inside pitch. From these results, we can conclude that the proposed method estimated the 3D trajectory of the CoM in an active sport scene without requiring the installation of devices, such as force plates, into the field or requiring the subject to wear any electronic devices.

[2] https://www.xsens.com/products/xsens-mvn-analyze/.

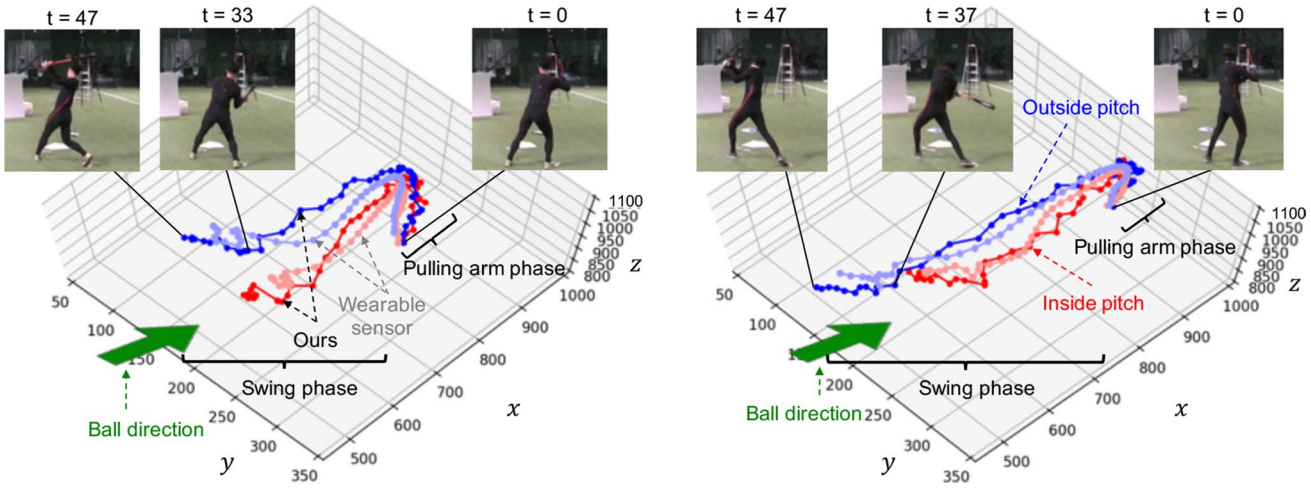

Fig. 7 Experimental results concerning the transition of the CoM while baseball players swung against "inside (red)" and "outside (blue)" balls. The red and blue trajectories are the CoM transitions estimated by the proposed method, and the light red and blue trajectories show the CoM calculated from the wearable sensor data. The left graph shows the CoM transition while the professional player swung, and the right graph shows the CoM transition of the amateur player's swings viewed from above

5 Discussion

When estimating the CoM using the proposed method, the number of cameras affects the accuracy of both the 3D human body reconstruction and the 3D kinematic estimation. We examined the relationship between the number of cameras and the estimated CoM accuracy, which was evaluated by a comparison to the CoP, as in the experiment in Sect. 4.1. In our method, since all joints must be detected with two or more cameras, when cameras that do not satisfy the conditions were selected, we manually complemented the undetected joints manually.

Figure 8 shows the error between the CoP and the vertically projected CoM in each static posture when the number of cameras was changed from two to five. Figure 8 also depicts the average and standard deviations of each possible combination of cameras. It can be seen that the average error increased gradually as the number of cameras decreased from five to three, but when the CoM was estimated using only two cameras, the CoM precision dropped dramatically. The estimation accuracy of the CoM depends on the accuracy of the human model created with visual hull. The number and arrangement of cameras in visual hull-based human motion tracking have been explored by Corraza et al. [10]. Modifying camera configurations by referring to their conclusion would improve the accuracy of CoM estimation.

While the current study segmented the body into nine parts, for further improvement in accuracy, more categories will be needed, such as hair, clothes, shoes, tools, fat, bones, and muscles. In practice, we consider that fitting the available anatomy models to the subject will lead to a higher reliability.

Further investigation is needed on whether we should include tools held by subjects in CoM calculations (e.g., a bat, a racket, a golf club) from the viewpoint of sports data analysis as well as how the difference appears in the CoM estimation. Note that in the present study, we removed the bat to obtain the CoM of the subject only, shown in Fig. 7, by masking the bat out in the proposed pipeline, as described in Sect. 3.2. When a bat or a racket is segmented in a multi-view set of cameras, the tool is three-dimensionally tracked and we obtain the motion of it.

As the first step of our research, we assumed one subject in a scene. If we take multiple subjects into consideration, this will require an extension to separate each person in a voxel space. While the CNN-based bone estimation [5] can handle multiple persons in a single view, the proposed

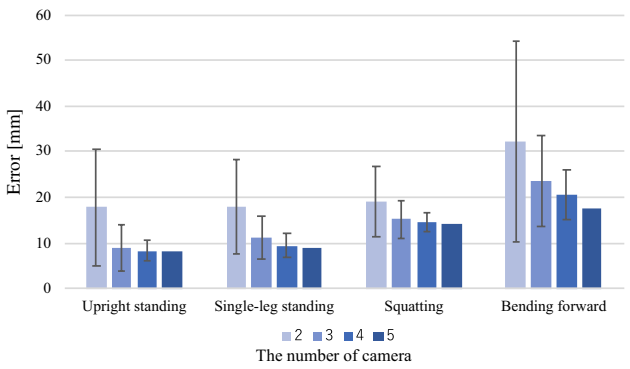

Fig. 8 The error between the reference value and the vertically projected CoM, estimated using different numbers of cameras

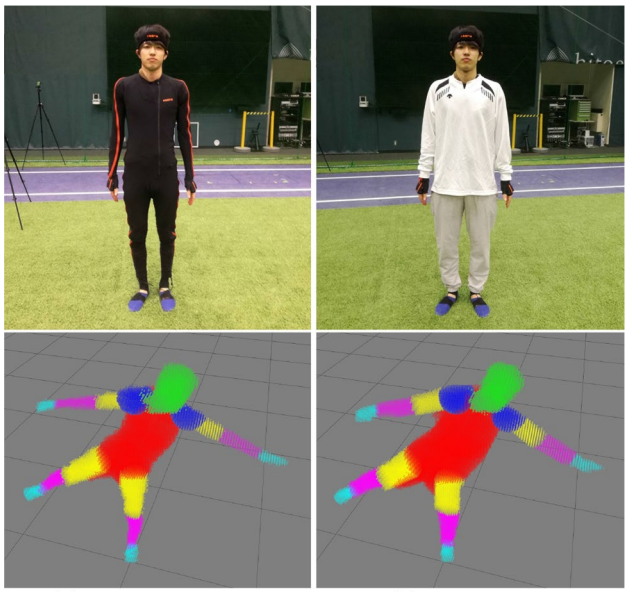

(a) Form-fitting clothes **(b)** Loose clothes

Fig. 9 A comparison of the appearance between the subjects wearing form-fitting and loose clothes

method requires the identification of persons in multiple images, which will necessitate additional efforts.

The proposed method estimates the CoM as the gravity point of a set of voxels. Therefore, it can be supposed that clothes may affect its performance since the subject's silhouette changes. Here, we additionally demonstrate the effects of clothes on the proposed method.

As shown in the first row of Fig. 9, we utilized images from subjects wearing both form-fitting and loose clothing as the input for the proposed method. From the second row of Fig. 9, we can see that the reconstructed 3D model with loose clothes was expanded compared to the subject wearing form-fitting clothes, even when the subject stood in the same posture. The quantitative results of such cases, utilizing the same configuration introduced in Sect. 4.1.1, show that the average error when the subjects wore loose clothes was 81% larger than in the case of wearing form-fitting clothes. These results reveal that the proposed method's accuracy degraded when the subject is wearing loose clothes. Therefore, reducing the effect of loose clothing on the method's accuracy is an aim of our future work.

6 Conclusion

This paper proposed a novel vision-based CoM estimation algorithm based on multi-view images for sports performance analysis. The key approach of the proposed method is to assign an appropriate weight to each voxel, reconstructed in a visual hull manner. Evaluations with real data demonstrated that the proposed method can estimate the CoM within errors of approximately 10 mm concerning the CoP compared to the data measured with force plates in static conditions. In addition, the proposed method reasonably estimated the 3D trajectory of the CoM in a dynamic scene.

Acknowledgements This work was supported by Grant-in-Aid for JSPS Fellows (19J22153).

References

1. Baumgartner RN, Chumlea WC, Roche AF (1989) Estimation of body composition from bioelectric impedance of body segments. Am J Clin Nutr 50(2):221–226
2. Brennan SM, Kollár L, Springer G (2003) Modelling the mechanical characteristics and on-snow performance of snowboards. Sports Eng 6(4):193–206
3. Bullas AM, Choppin S, Heller B, Wheat J (2016) Validity and repeatability of a depth camera-based surface imaging system for thigh volume measurement. J Sports Sci 34(20):1998–2004
4. Cao S, Chen K, Nevatia R (2016) Activity recognition and prediction with pose based discriminative patch model. In: 2016 IEEE winter conference on applications of computer vision (WACV), IEEE, pp 1–9
5. Cao Z, Simon T, Wei SE, Sheikh Y (2017) Realtime multi-person 2d pose estimation using part affinity fields. In: Computer vision and pattern recognition (CVPR), Hawaii, US
6. Carpentier J, Benallegue M, Mansard N, Laumond JP (2016) Center-of-mass estimation for a polyarticulated system in contact—a spectral approach. IEEE Trans Robot 32(4):801–822
7. Chew DK, Ngoh KJH, Gouwanda D, Gopalai AA (2018) Estimating running spatial and temporal parameters using an inertial sensor. Sports Eng 21(2):115–122
8. Clarkson S, Wheat J, Heller B, Choppin S (2016) Assessment of a microsoft kinect-based 3d scanning system for taking body segment girth measurements: a comparison to ISAK and ISO standards. J Sports Sci 34(11):1006–1014
9. Corazza S, Muendermann L, Chaudhari A, Demattio T, Cobelli C, Andriacchi TP (2006) A markerless motion capture system to study musculoskeletal biomechanics: visual hull and simulated annealing approach. Ann. Biomed. Eng. 34(6):1019–1029
10. Corazza S, Mündermann L, Gambaretto E, Ferrigno G, Andriacchi TP (2009) Markerless motion capture through visual hull, articulated ICP and subject specific model generation. Int J Comput Vis 87(1):156. https://doi.org/10.1007/s11263-009-0284-3
11. Dawes R, Mann M, Weir B, Pike C, Golds P, Nicholson M (2012) Enhancing viewer engagement using biomechanical analysis of sport. In: Proc. of the NEM Summit, pp 121—126
12. Drücker S, Schneider K, Ghothra NK, Bargmann S (2018) Finite element simulation of pole vaulting. Sports Eng 21(2):85–93
13. González A, Hayashibe M, Fraisse P (2012) Estimation of the center of mass with Kinect and Wii balance board. In: 2012 IEEE/RSJ International Conference on Intell. Robots and Systems (IROS), IEEE, pp 1023–1028
14. González A, Hayashibe M, Bonnet V, Fraisse P (2014) Whole body center of mass estimation with portable sensors: using the statically equivalent serial chain and a Kinect. Sensors 14(9):16955–16971
15. Göpfert C, Pohjola MV, Linnamo V, Ohtonen O, Rapp W, Lindinger SJ (2017) Forward acceleration of the centre of mass

during ski skating calculated from force and motion capture data. Sports Eng 20(2):141–153
16. Hale SA, Hertel J, Olmsted-Kramer LC (2007) The effect of a 4-week comprehensive rehabilitation program on postural control and lower extremity function in individuals with chronic ankle instability. J Orthop Sports Phys Ther 37:303–311
17. Hrysomallis C (2011) Balance ability and athletic performance. Sports Med 41(3):221–232
18. Imamura RT, Hreljac A, Escamilla RF, Edwards WB (2006) A three-dimensional analysis of the center of mass for three different judo throwing techniques. J Sports Sci Med 5:122–131
19. Kobayashi N, Sato S, Matsuzaki Y, Nakamura A (2017) Basic study on appearance-based proficiency evaluation of the football inside kick. In: 2017 26th IEEE international symposium on robot and human interactive communication (RO-MAN), IEEE, pp 1234–1239
20. de Leva P (1996) Adjustments to zatsiorsky-seluyanov's segment inertia parameters. J Biomech 29(9):1223–1230
21. Mapelli A, Zago M, Fusini L, Galante ACD, Sforza C (2014) Validation of a protocol for the estimation of three-dimensional body center of mass kinematics in sport. Gait Posture 39(1):460–465
22. Martin WN, Aggarwal JK (1983) Volumetric descriptions of objects from multiple views. IEEE Trans Pattern Anal Mach Intell 2:150–158
23. Mundermann L, Corazza S, Chaudhari AM, Alexander EJ, Andriacchi TP (2005) Most favorable camera configuration for a shape-from-silhouette markerless motion capture system for biomechanical analysis. https://doi.org/10.1117/12.587970
24. Mündermann L, Corazza S, Andriacchi TP (2006) The evolution of methods for the capture of human movement leading to markerless motion capture for biomechanical applications. J Neuroeng Rehabilit 3(1):6
25. Najafi B, Lee-Eng J, Wrobel JS, Goebel R (2015) Estimation of center of mass trajectory using wearable sensors during golf swing. J Sports Sci Med 14(2):354–363
26. Pai YC, Patton J (1997) Center of mass velocity-position predictions for balance control. J Biomech 30(4):347–354
27. Saini M, Kerrigan DC, Thirunarayan MA, Duff-Raffaele M (1998) The vertical displacement of the center of mass during walking: a comparison of four measurement methods. J Biomech Eng 120(1):133–139
28. Sheets AL, Abrams GD, Corazza S, Safran MR, Andriacchi TP (2011) Kinematics differences between the flat, kick, and slice serves measured using a markerless motion capture method. Ann Biomed Eng 39(12):3011
29. Takeda K, Mani H, Hasegawa N, Sato Y, Tanaka S, Maejima H, Asaka T (2017) Adaptation effects in static postural control by providing simultaneous visual feedback of center of pressure and center of gravity. J Physiol Anthropol 36(1):31
30. Tao W, Liu T, Zheng R, Feng H (2012) Gait analysis using wearable sensors. Sensors 12(2):2255–2283
31. Tsitsoulis A, Bourbakis NG (2015) A methodology for extracting standing human bodies from single images. IEEE Trans Hum Mach Syst 45:1–12
32. Welch CM, Banks SA, Cook FF, Draovitch P (2006) Hitting a baseball: a biomechanical description. J Orthop Sports Phys Ther 22(5):193–201
33. Wieber PB (2006) Holonomy and nonholonomy in the dynamics of articulated motion. In: Fast motions in biomech. and robotics. Springer, Berlin, pp 411–425
34. Winter DA, Patla AE, Frank JS (1990) Assessment of balance control in humans. Med Prog Technol 16(1):31–51
35. Zatsiorsky VM, King DL (1997) An algorithm for determining gravity line location from posturographic recordings. J Biomech 31(2):161–164
36. Zecha D, Einfalt M, Eggert C, Lienhart R (2018) Kinematic pose rectification for performance analysis and retrieval in sports. In: The IEEE conference on computer vision and pattern recognition (CVPR) workshops
37. Zhang Z (2000) A flexible new technique for camera calibration. IEEE Trans Pattern Anal Mach Intell 22(11):1330–1334